Quantifying Mapping Orbit Performance in the Vicinity of Primitive Bodies

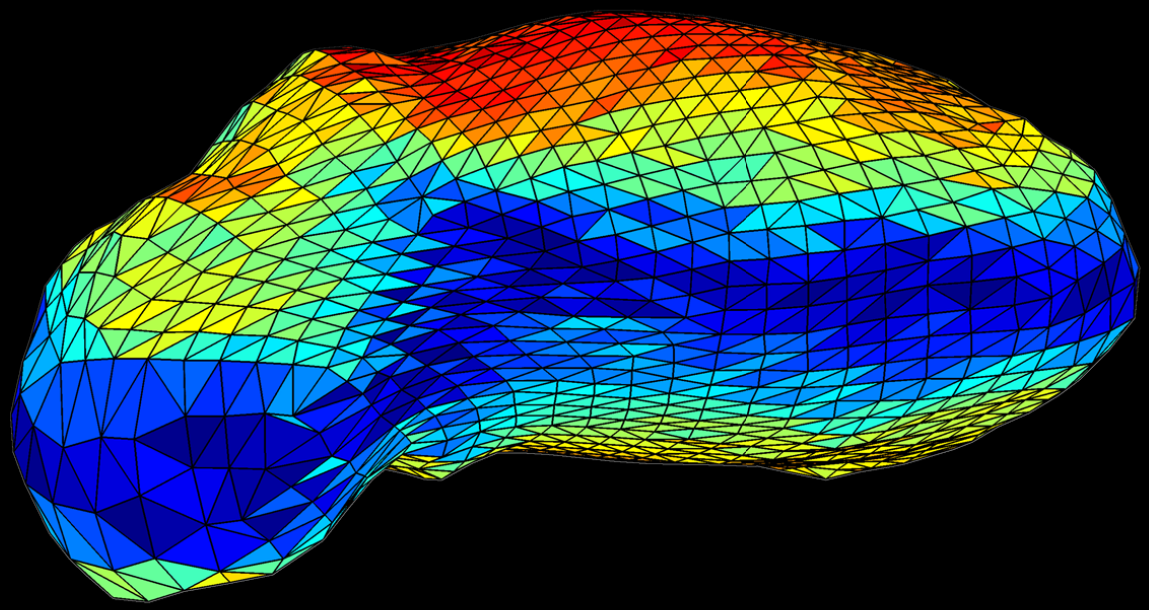

Thomas A. Pavlak, Stephen B. Broschart, and Gregory Lantoine

Jet Propulsion Laboratory, California Institute of Technology
Pasadena, California

© 2015 California Institute of Technology. Government sponsorship acknowledged.

Introduction

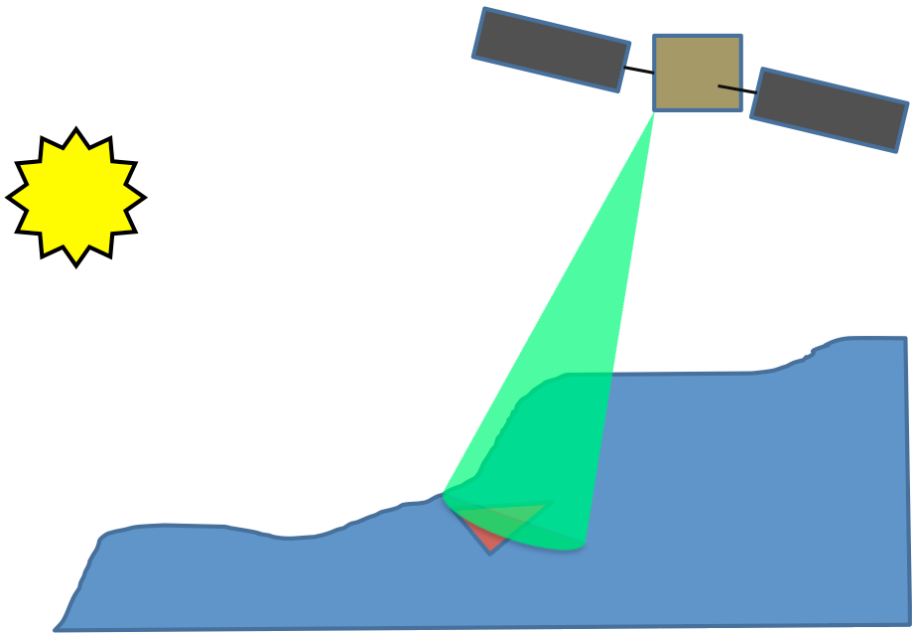

- Predicting and quantifying mapping orbit capability near primitive bodies is nontrivial
  - Complex dynamics and orbit geometries
  - Irregular shape of primitive bodies
- JPL-developed software leveraged to design various candidate mapping orbits and compute wealth of surface observation information
- Quantitative metrics and visualization utilized to assess effectiveness of each candidate trajectory
  - Metrics of interest include surface area coverage, lighting conditions, and variety of viewing angles achieved
  - Intended to help mission designers make more informed decisions during preliminary mission formulation activities

Remote Sensing Geometry

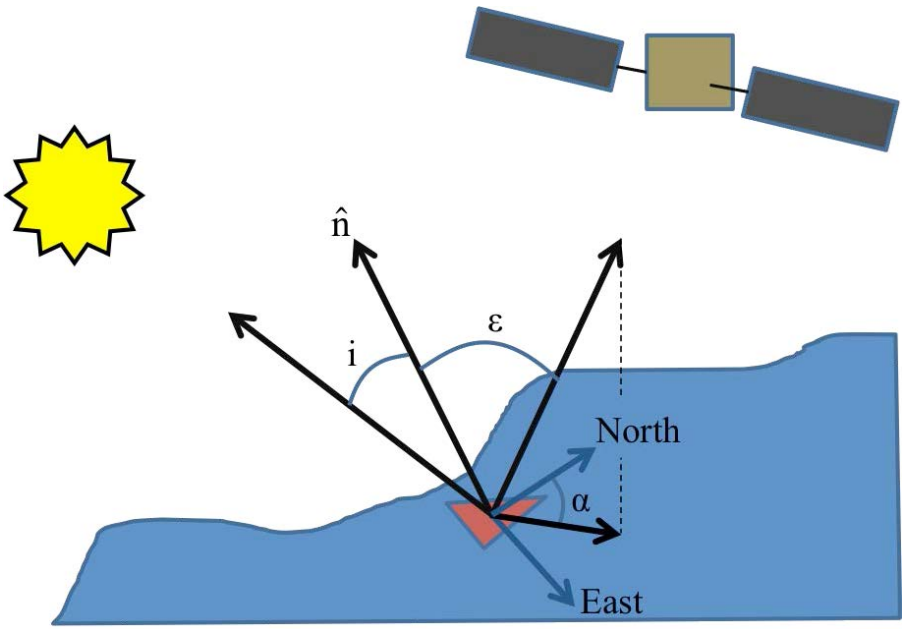

- **Important parameters:**
  - Spacecraft azimuth angle, α
    - Spacecraft observation angle wrt due north
  - Incidence angle, *i*
    - Angle between surface normal and Sun line
  - Emission angle, ε
    - Angle between surface normal and spacecraft line
  - Phase angle, ϕ
    - Primitive body-Sun-spacecraft angle
  - Spacecraft range, *r*
    - Primitive body-spacecraft distance

- **For surface mapping activities, it is desirable to observe the body with a *variety* of observation geometries, ranges, and lighting conditions**

Observation Geometry Constraints

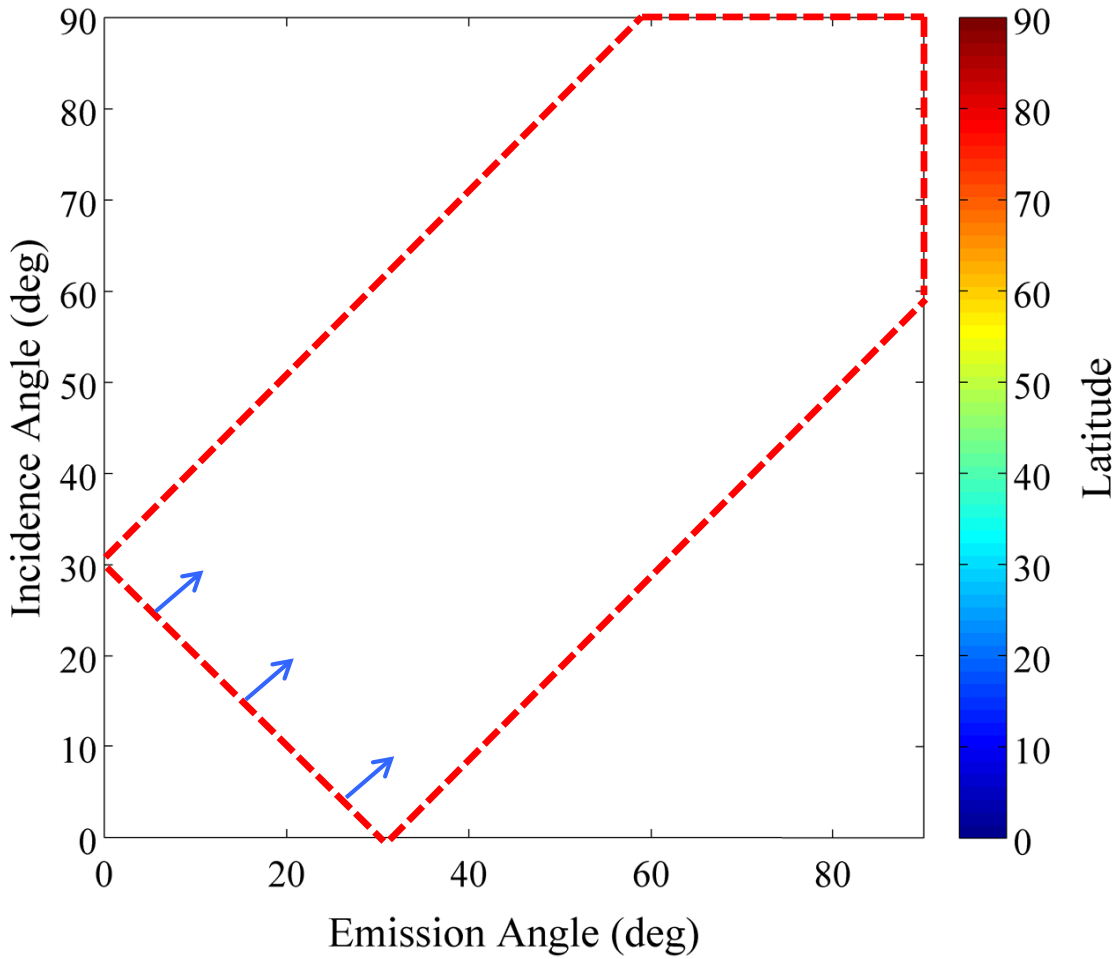

- As the radius of the primitive body goes to zero, the phase, incidence, and emission angles are related by:

$$|i - \epsilon| \leq \phi \leq i + \epsilon$$

- This constraint implies the following:

$$\boxed{\epsilon \geq \phi - i}$$

$$\epsilon \geq i - \phi, \text{ if } (i - \epsilon) \geq 0$$

$$\epsilon \leq i + \phi, \text{ if } (i - \epsilon) < 0$$

- Outer incidence-emission envelope governed by phase angle → function of trajectory

Observation Geometry Constraints

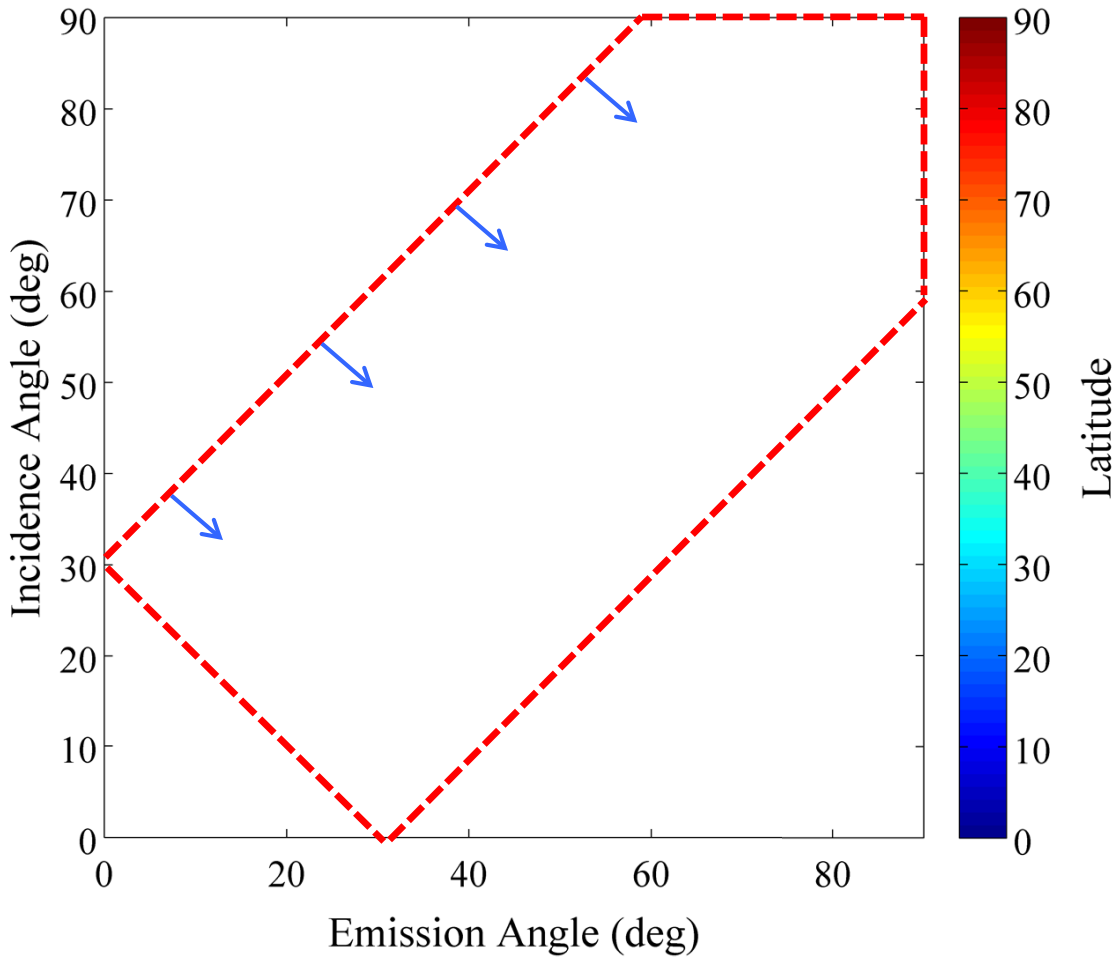

- As the radius of the primitive body goes to zero, the phase, incidence, and emission angles are related by:

$$|i - \epsilon| \leq \phi \leq i + \epsilon$$

- This constraint implies the following:

$$\epsilon \geq \phi - i$$

$$\boxed{\epsilon \geq i - \phi, \text{ if } (i - \epsilon) \geq 0}$$

$$\epsilon \leq i + \phi, \text{ if } (i - \epsilon) < 0$$

- Outer incidence-emission envelope governed by phase angle → function of trajectory

Observation Geometry Constraints

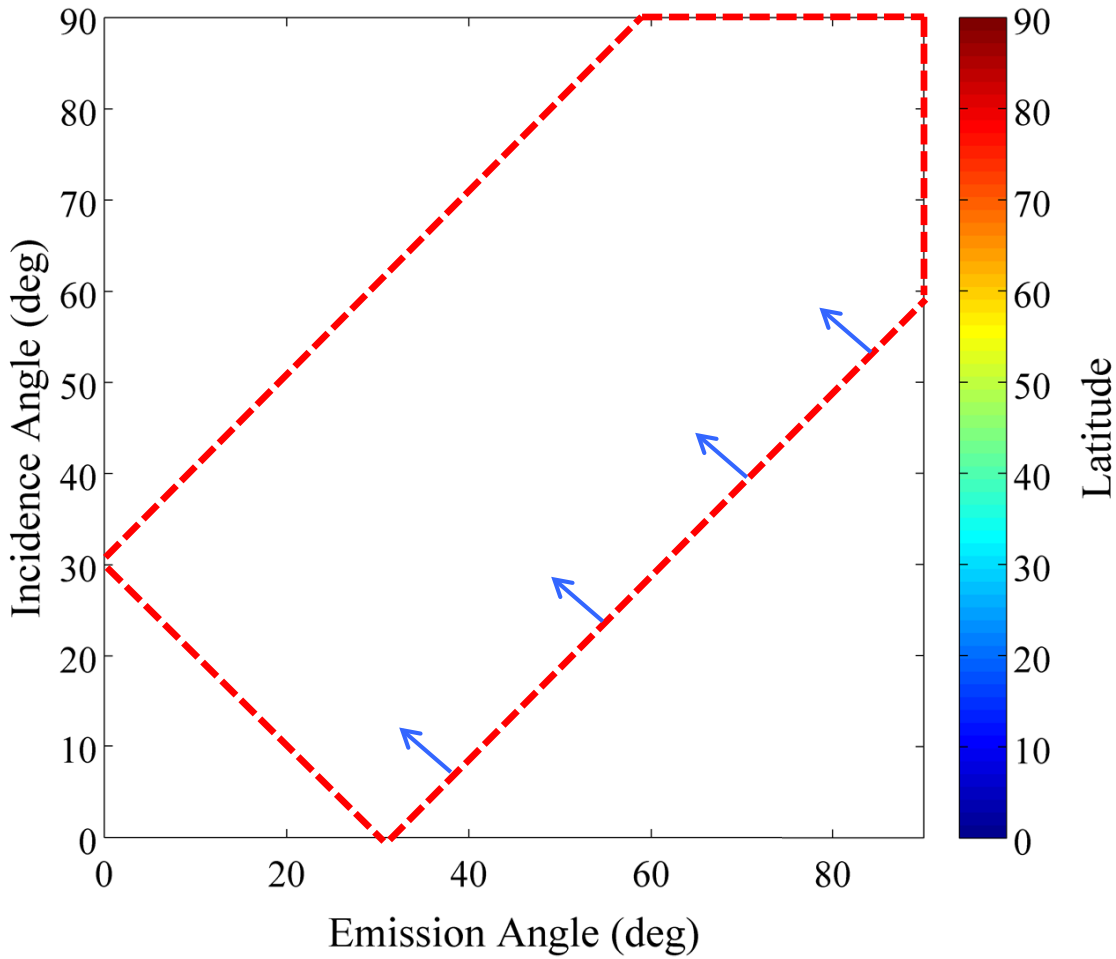

- As the radius of the primitive body goes to zero, the phase, incidence, and emission angles are related by:

$$|i - \epsilon| \leq \phi \leq i + \epsilon$$

- This constraint implies the following:

$$\epsilon \geq \phi - i$$

$$\epsilon \geq i - \phi, \text{ if } (i - \epsilon) \geq 0$$

$$\boxed{\epsilon \leq i + \phi, \text{ if } (i - \epsilon) < 0}$$

- Outer incidence-emission envelope governed by phase angle → function of trajectory

Observation Geometry Constraints

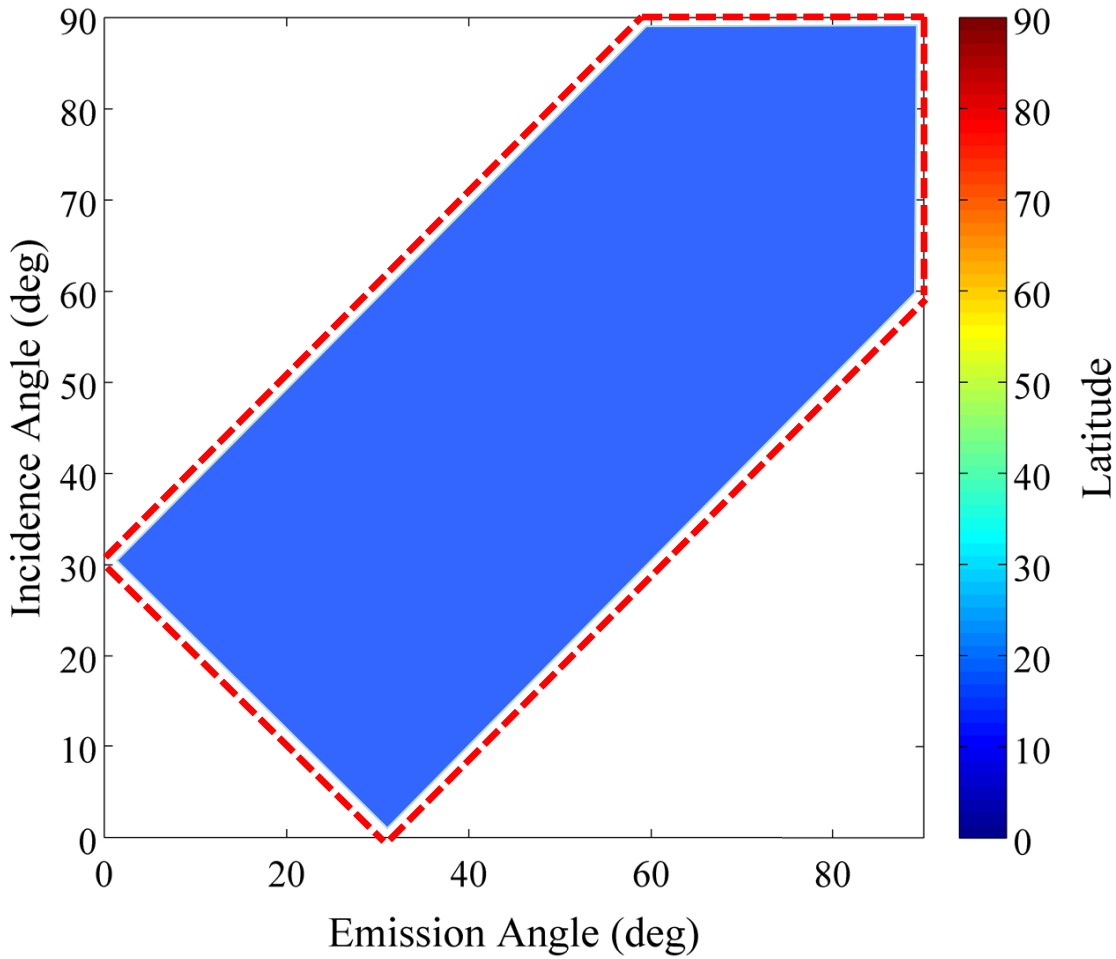

- As the radius of the primitive body goes to zero, the phase, incidence, and emission angles are related by:

$$|i - \epsilon| \leq \phi \leq i + \epsilon$$

- This constraint implies the following:

$$\epsilon \geq \phi - i$$

$$\epsilon \geq i - \phi, \text{ if } (i - \epsilon) \geq 0$$

$$\epsilon \leq i + \phi, \text{ if } (i - \epsilon) < 0$$

- Outer incidence-emission envelope governed by phase angle → function of trajectory
- Interior incidence emission structure governed by pole/shape → function of primitive body

Observation Geometry Constraints

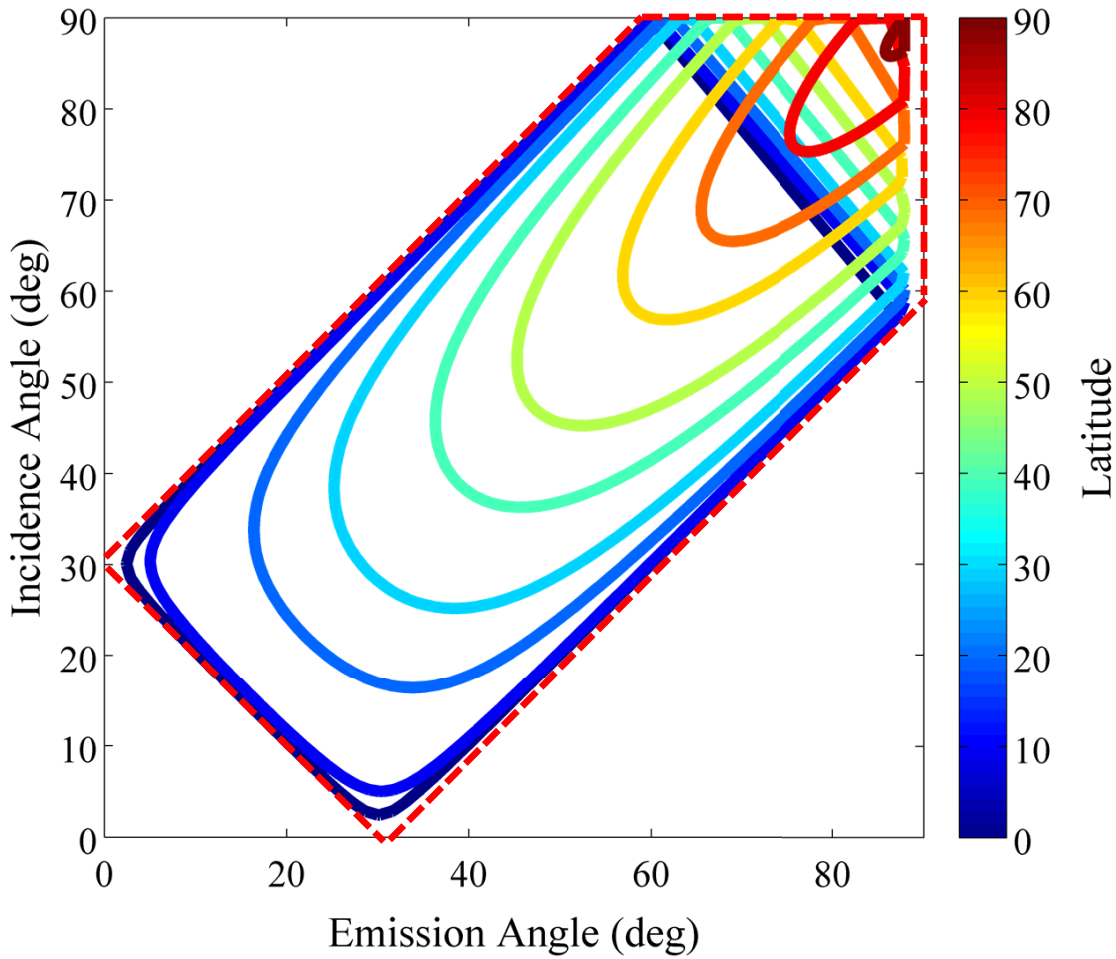

- As the radius of the primitive body goes to zero, the phase, incidence, and emission angles are related by:

$$|i - \epsilon| \leq \phi \leq i + \epsilon$$

- This constraint implies the following:

$$\epsilon \geq \phi - i$$

$$\epsilon \geq i - \phi, \text{ if } (i - \epsilon) \geq 0$$

$$\epsilon \leq i + \phi, \text{ if } (i - \epsilon) < 0$$

- Outer incidence-emission envelope governed by phase angle → function of trajectory
- Interior incidence emission structure governed by pole/shape → function of primitive body

Orbital Observation Strategies

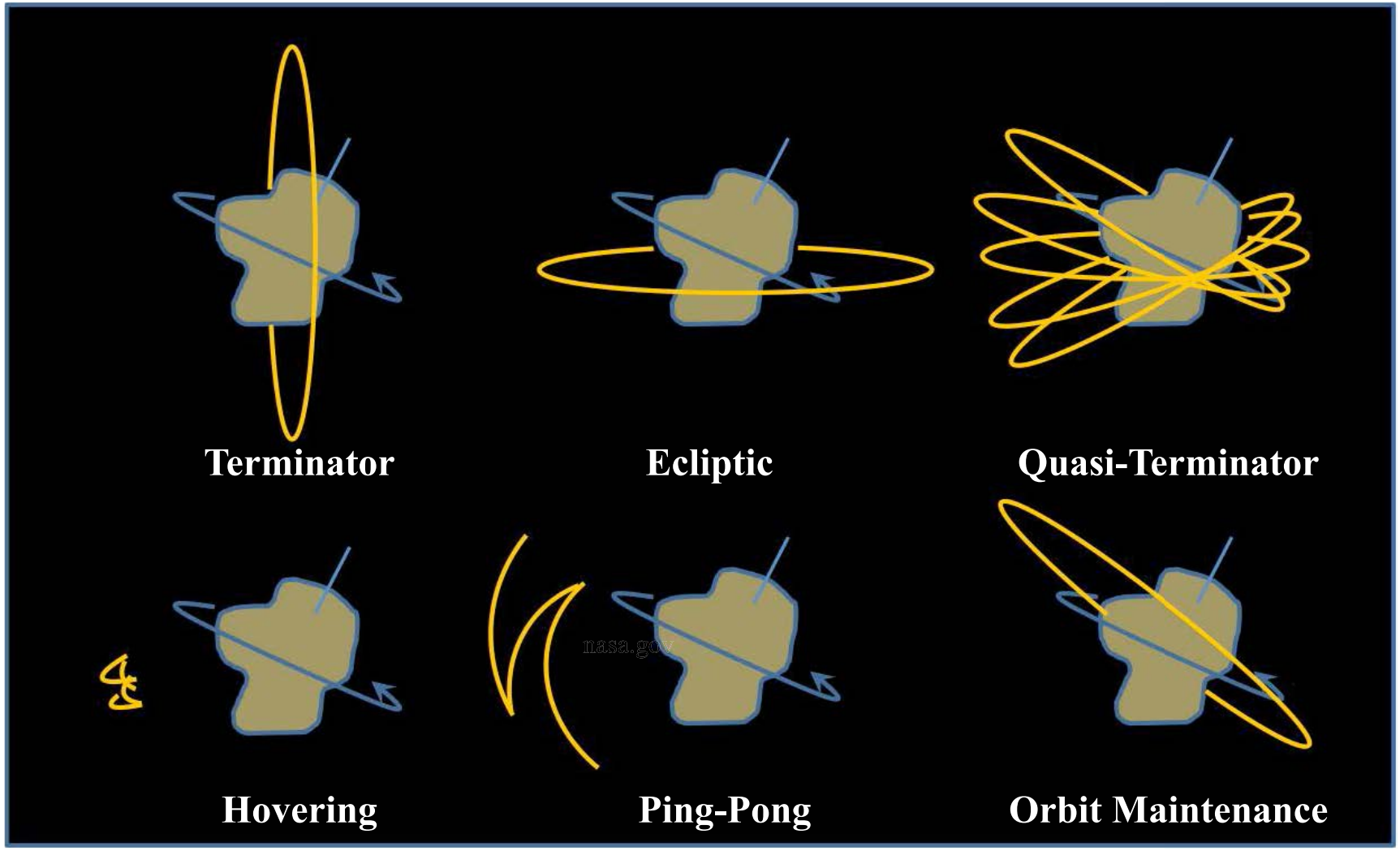

Computing Primitive Body Coverage

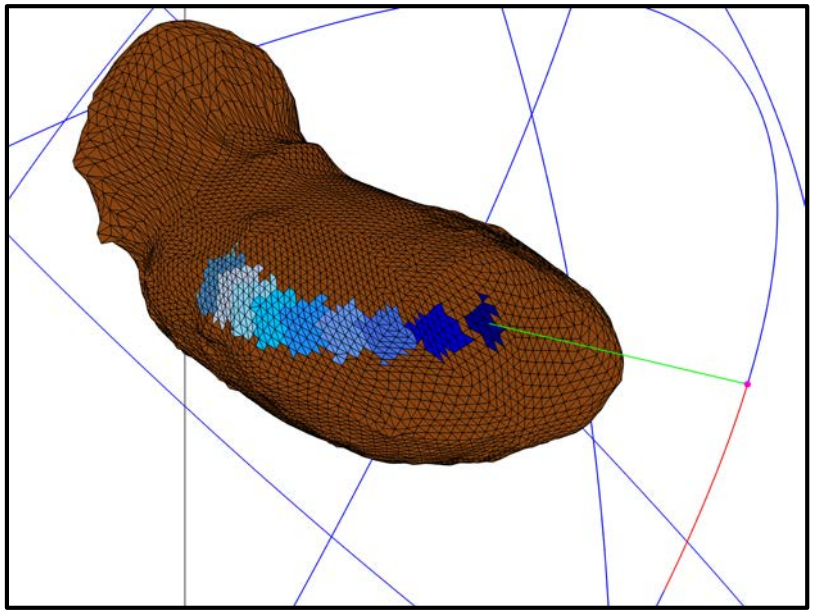

Example observation sequence along a polyhedral representation of Itokawa

- **Small Body Dynamics Toolkit (SBDT)**
  - Supplies primitive body shape and gravity models
    - Augmented circular restricted three-body problem used in this analysis (CR3BP + solar radiation pressure)
  - Represents body as triangular-faceted polyhedron
  - Contains tools to design "common" primitive body orbits

- **Primitive Body Coverage and Geometry Evaluator (PB-CAGE)**
  - Add-on for SBDT
  - Handles self-obstruction and self-shadowing
  - User-provided input:
    - Primitive body trajectory
    - Spacecraft trajectory and pointing
    - Instrument properties
    - Sequence of observation epochs
  - PB-CAGE-computed output (at each observation epoch):
    - Visible facets
    - Lighting conditions
    - Variety of observation properties including angles, range, surface resolution, etc.

Assumptions

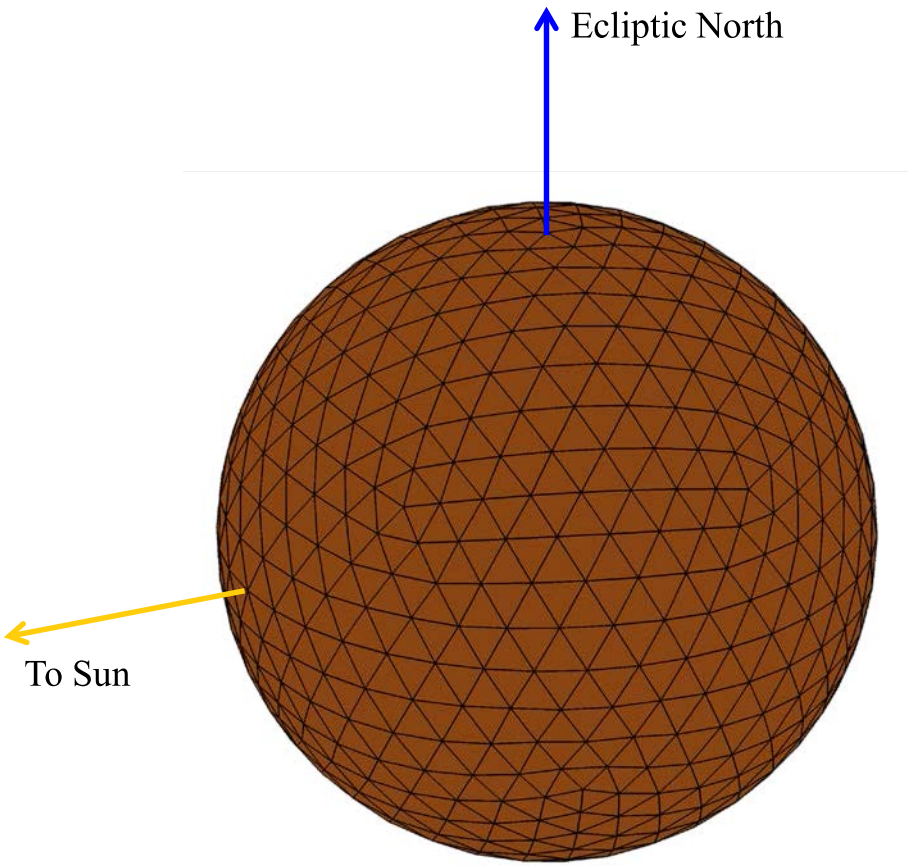

- **Spacecraft assumptions:**
  - Infinite instrument field-of-view
  - Instrument can observe body at any time
  - Angles computed with respect to facet centers
- **Primitive body assumptions:**
  - Spherical, triangular-faceted polyhedron
  - If greater than half of a facet is visible, then that entire facet is considered visible
  - Pole of the primitive body is *fixed* for the duration of each simulation

Assumptions
Pole Definitions

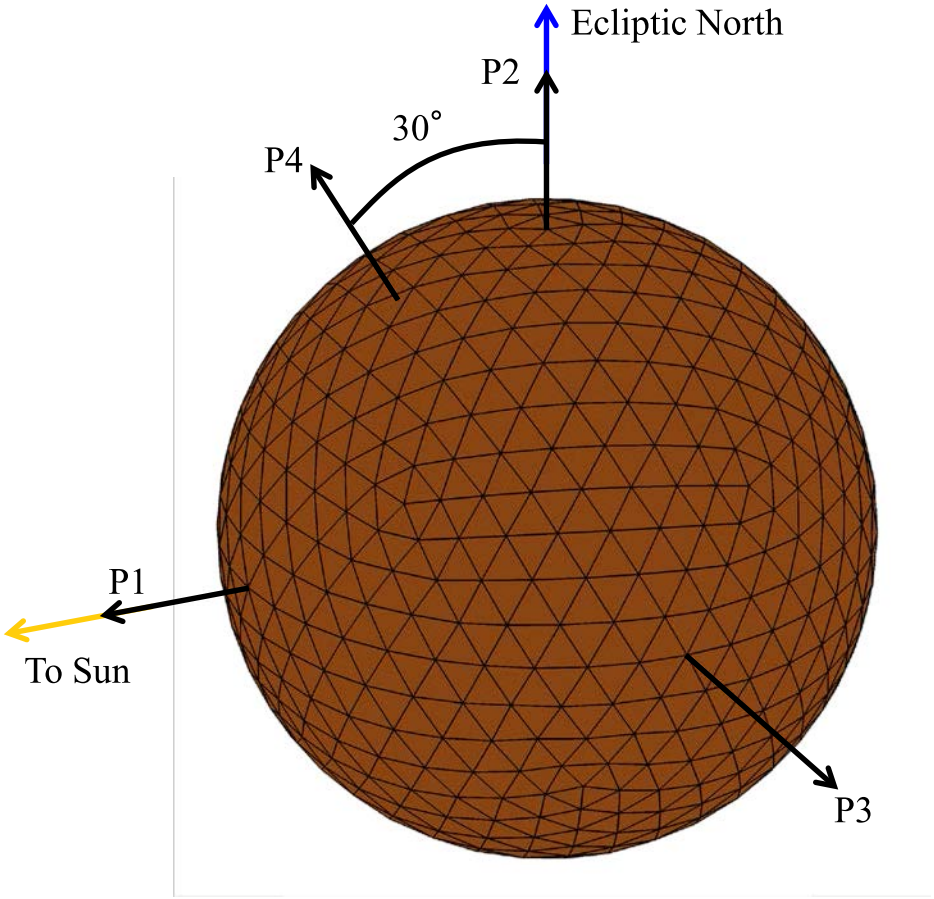

- **Four poles considered in this analysis:**
  - P1 aligned with body-Sun direction
  - P2 aligned with ecliptic north
  - P3 = P1 x P2
  - P4 is a 30 degree rotation of P2 vector about P3

Results

Terminator Orbits

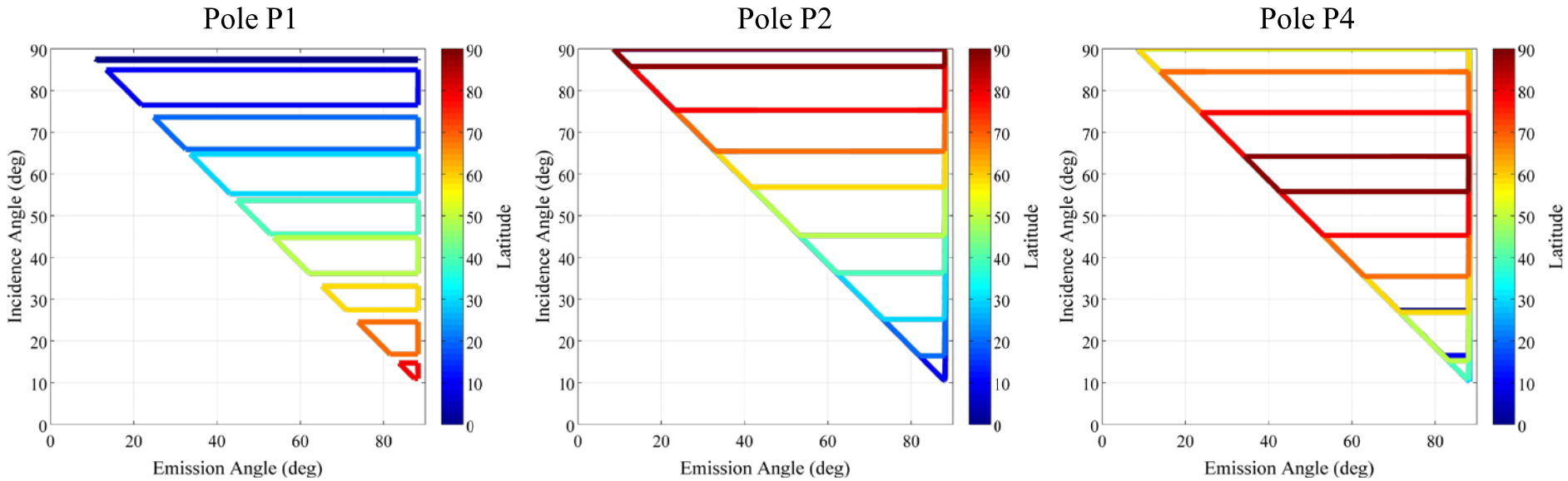

- Phase angle always greater than 90°
  - Relatively limited in incidence emission space
- Self-obstruction limits view of subsolar point
- For Pole P1, results are banded since each latitude is at constant incidence angle
  - Regions appear as polygons due to ±5° latitude binning
- For Pole P2, widest range of emission angle available near polar region

Results

Ecliptic Orbits

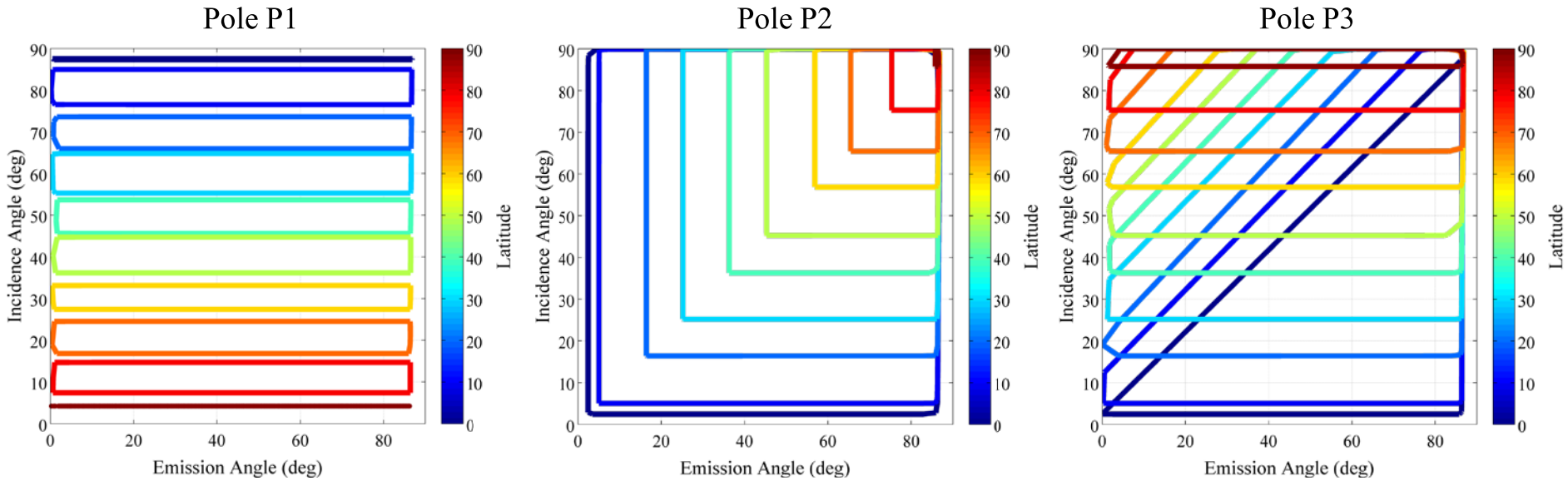

- Full range of phase angle achieved
  - Results in near complete coverage of incidence-emission space
  - Generally, coverage is best at low-to-mid latitudes
- Banded regions for Pole P1
- Poles P2 and P3 exhibit good coverage near equator
  - Self-obstruction can occur near ecliptic northern/southern regions
  - Little to no coverage near poles

Results

Quasi-Terminator Orbits

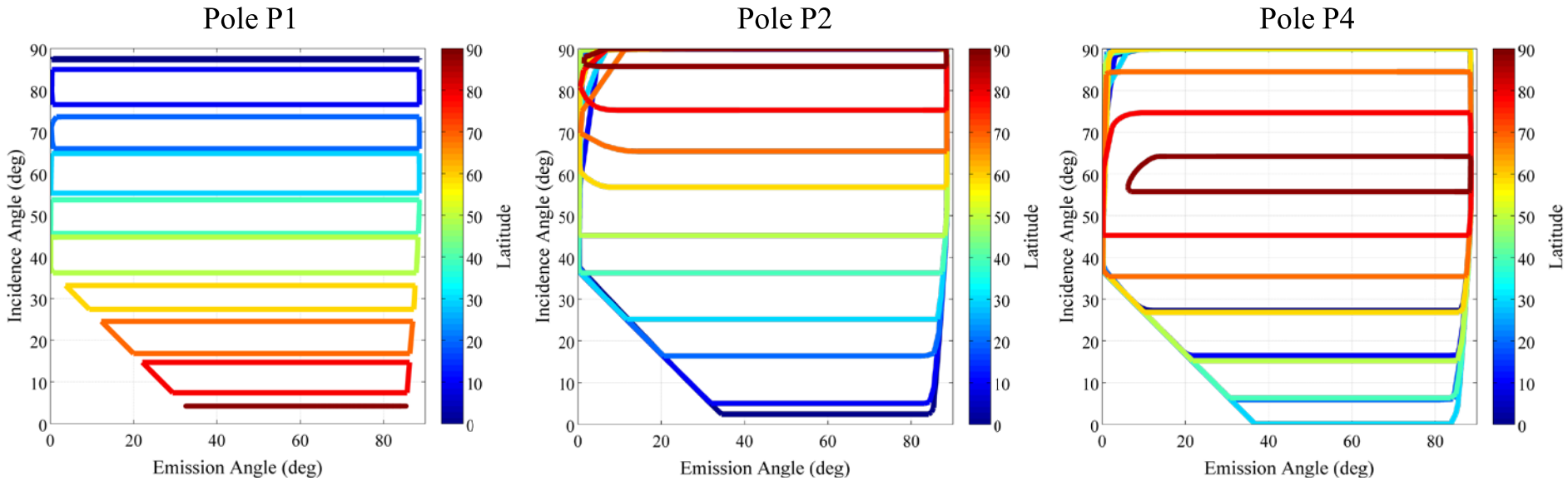

- Provide good coverage of incidence-emission space
- Similar to terminator orbits
  - Limited by minimum phase angle in lower-left corner of plot
  - Minimum phase angle generally much lower than terminator orbits
  - However, quasi-terminators can take longer to progress through range of viewing geometries
- For Pole P4, incidence-emission regions are "centered" around incidence angle equal pole declination (60°)

Results
Hovering

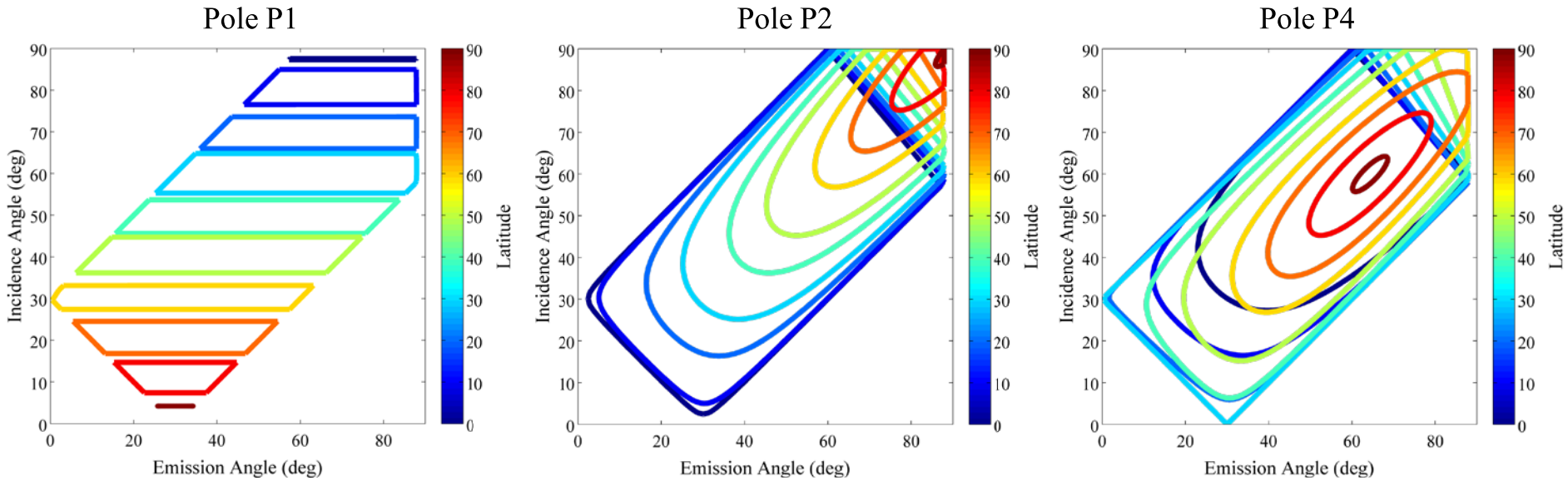

- Infinite hovering trajectories available
  - Assuming adequate spacecraft maneuvering and operational capability
- Ecliptic hovering 30° off of body-Sun line depicted here (constant 30° phase angle)
  - Phase-incidence-emission constraints clearly visible
- For Pole P2, coverage is significantly better at low latitudes than near the poles
- For Pole P4, polar coverage is only available near declination of the pole (60°)

Results

Ping-Pong Orbits

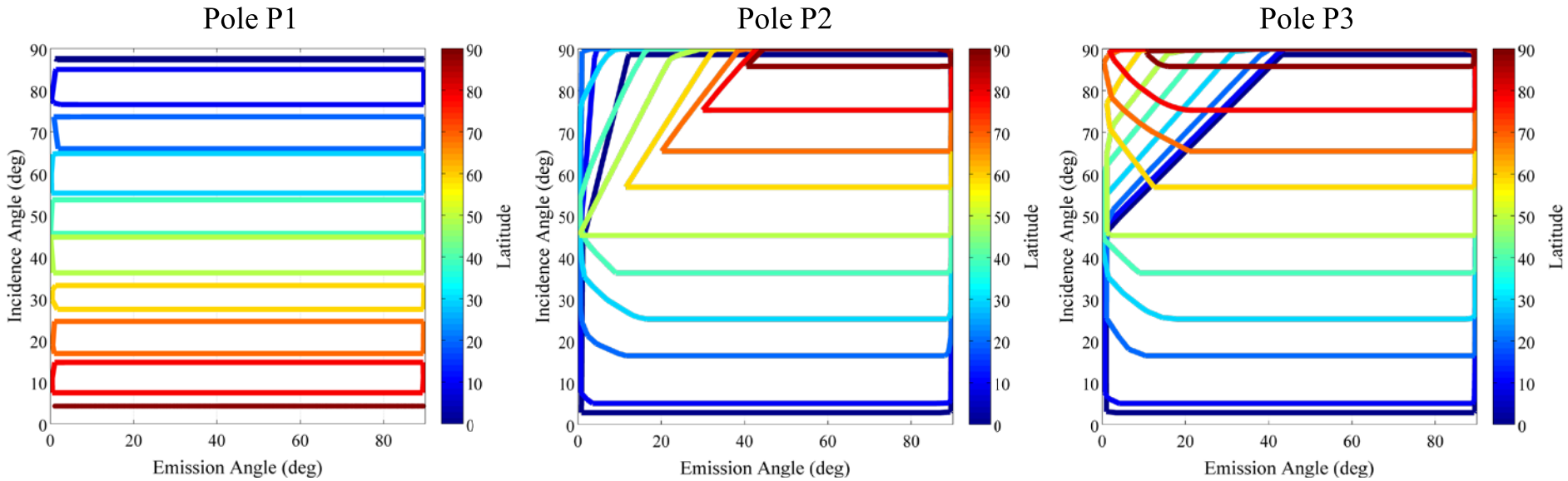

- Infinite ping-pong trajectories available
  - Assuming adequate spacecraft maneuvering and operational capability
- Any possible viewing geometry can be achieved at the cost of fuel and mission complexity
- Arbitrary ping-pong presented here for illustration purposes

Case Study

Primitive Body and Spacecraft Definitions

- **Primitive Body Definition**
  - Normalized acceleration, $\beta = 25$, assumed
  - Given constants and spacecraft properties, primitive body gravitational parameter determined by

$$\beta = \frac{G_1}{\left(\frac{m}{A}\right)\mu_S^{2/3}\mu_{PB}^{1/3}}$$

$$G_1 = 1 \times 10^{14}\frac{\mathrm{kg}\cdot\mathrm{km}}{\mathrm{s}^2}$$

$$\mu_S = 1.327 \times 10^{11}\frac{\mathrm{km}^3}{\mathrm{s}^2}$$

    - $\mu_{PB} = 1.3415 \times 10^{-8}\ \mathrm{km}^3/\mathrm{s}^2$
  - Spherical, phase-locked primitive body with uniform density of 1 g/cm^2 also assumed
    - $r = 363$ km
    - 1,280 facets used in polyhedral mesh

- **Spacecraft Definition**
  - Representative values of mass and cross-sectional area

$$m = 1100\ \mathrm{kg}$$

$$A = 14\ \mathrm{m}^2$$

Case Study
Example Orbits

- **Five Example Orbits Considered**
  - Quasi-terminator orbit
    - Light-side QTO
  - Terminator orbit
  - Ping-pong orbit
  - Ecliptic orbit
    - Non-ballistic
  - Hover orbit
    - 10 km subsolar
- **ACR3BP dynamics**
  - Plot shown in Sun-body rotating frame

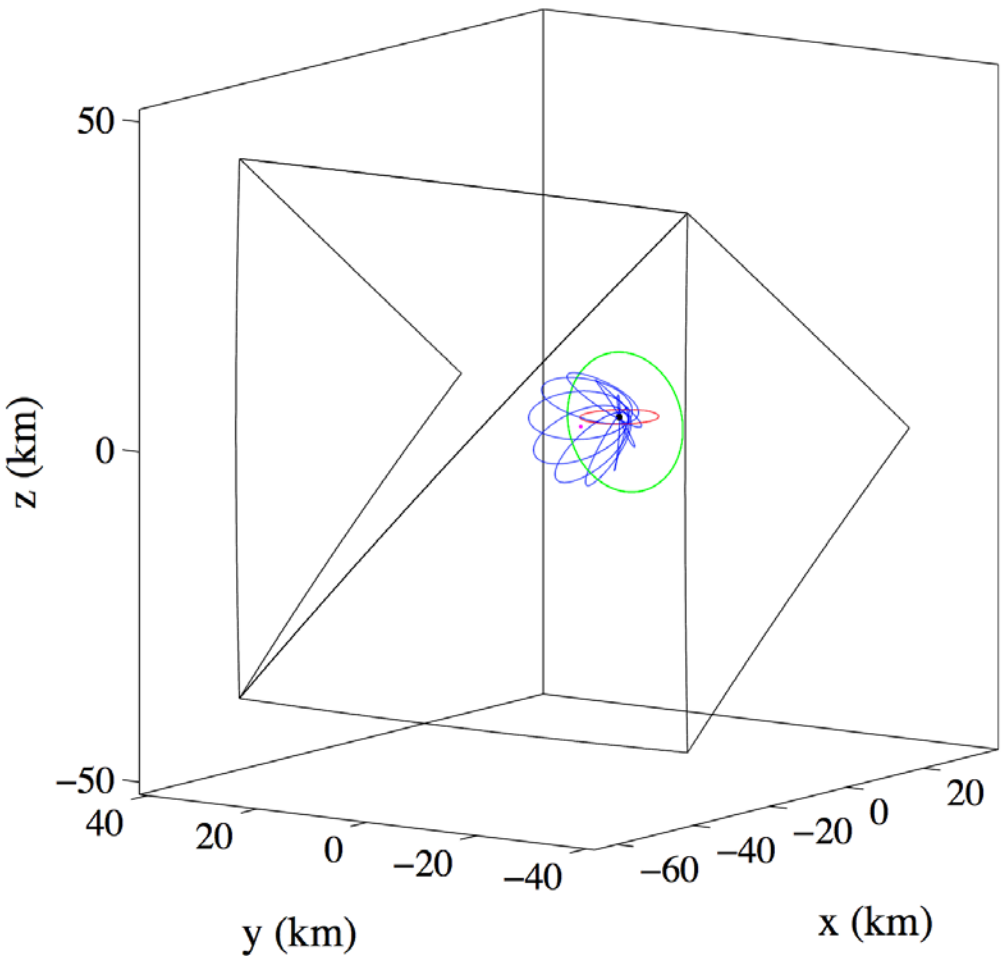

Case Study

Mapping Metrics Considered

- **Orbital period**
  - Yields insight into observation repeat time and total duration required to complete mapping
- **Percentage of surface area coverage achieved in one period**
  - Related to time required to complete mapping
- **Mean spacecraft range**
  - How close, on average, a spacecraft is to the body relates to surface resolution, etc.
- **Minimum phase angle**
  - Bounds incidence-emission space and describes how close the spacecraft passes to subsolar
- **Range at minimum phase angle**
  - Lower ranges at minimum solar phase angle are generally preferable
- **Mean and standard deviation of phase angle**
  - Typical phase angle provided by orbit
  - Gives insight to variety of phase angles achieved
- **Standard deviation of mean emission angle**
  - Incidence angle fixed for phase-locked body
  - Represents amount of variety in observation geometry across polyhedral facets
- **Frequency of required maneuvers**
  - Related to fuel consumption and operational complexity of candidate orbit

Case Study

Results

	Period (days)	% Coverage (1 period)	Mean Range (km)	Min. Φ (deg)	Range at Min. Φ (km)	Mean Φ (deg)	std Φ (deg)	std mean emission (deg)	Mnvr Freq.
QTO	113.02	50.91	10.94	36.77	13.62	49.85	20.91	4.14	N/A
Terminator	21.91	50.09	10.7	98.38	10.54	98.42	0.0296	11.27	N/A
Ping Pong	73.33	50.91	56.95	6.33	43.57	53.62	21.96	4.59	x 10 days
Equatorial	9	50.91	5.91	7.7	6	90.81	53.56	11.06	x 5 days
Hover	45	48.5	10	0	10.04	0	0	21.23	Cont.

- Minimum phase angle
  - Low for ping-pong, ecliptic, and hover orbits
  - Near polar for terminator
  - QTO consistent with user-defined orbit parameters
- Standard deviation of phase and mean emission angles
  - Large std(ϕ) and std(mean(ε)) for ecliptic orbit → wide range of phase angle, little variation in viewing geometry near poles
  - Small std(ϕ) for terminator → trajectory is nearly polar
  - QTO and ping-pong exhibit larger std(ϕ) and lower std(mean(ε)) → both positive; variety of observations across body
- Maneuver frequency
  - QTO and terminator are stable, others require regular maneuvers (near-constant maneuvering for "true hover")

Case Study

Results – Mean Emission Angle

- **Visualization confirms metrics in previous table**
- Smaller std(mean(ε)) for QTO and ping-pong orbits
  - Similar mean(ε) across all facets
- Larger std(mean(ε)) for other three orbits
  - Implies variety of observation geometry not consistent across body
  - Terminator has poor coverage near subsolar point
  - Ecliptic orbit has poor coverage near poles
  - Hover orbit has poor coverage near terminator

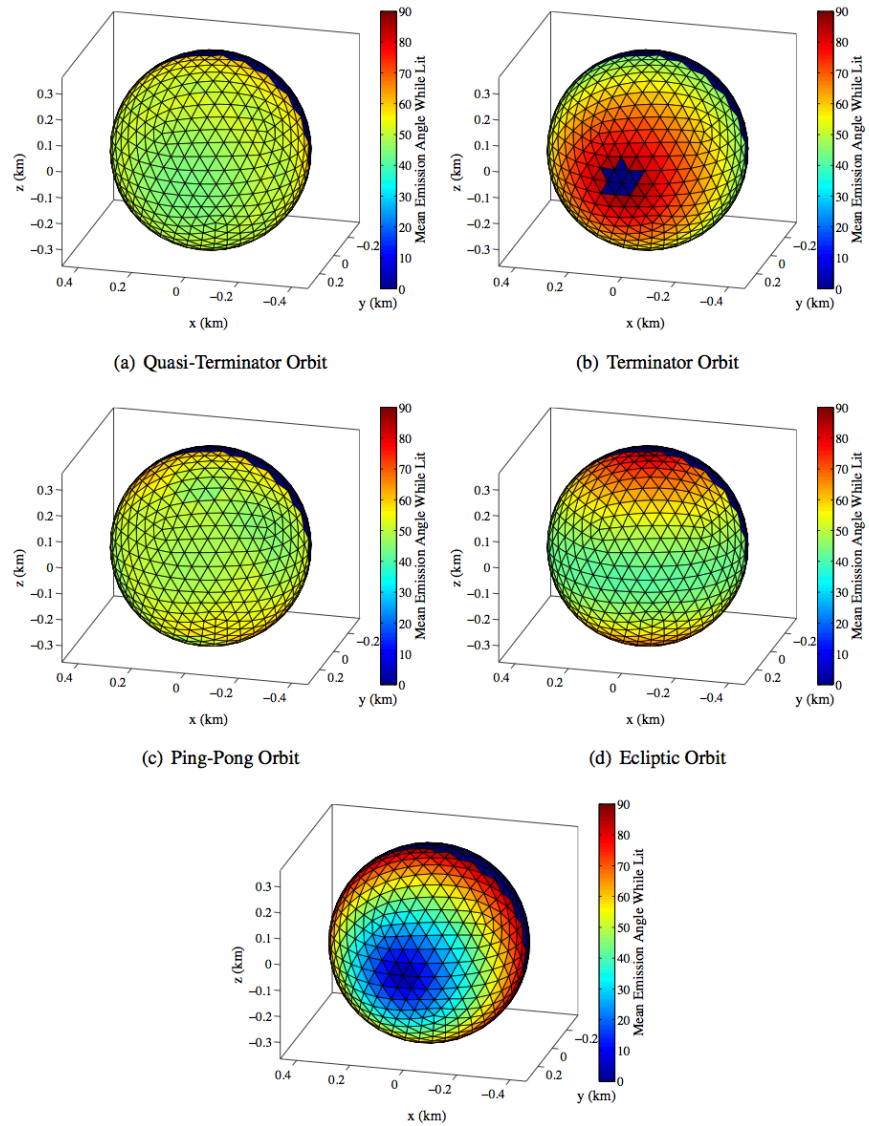

(a) Quasi-Terminator Orbit (b) Terminator Orbit (c) Ping-Pong Orbit (d) Ecliptic Orbit (e) Hover Orbit

Concluding Remarks

- Investigation intended to provide preliminary basis for comparison of candidate mapping orbits
- Emphasis on variety of observation geometry achieved
  - Phase-incidence-emission angle constraints strictly bound incidence-emission design space
  - Other relevant metrics certainly exist
- Results are generalized by use of a spherical primitive body with a fixed pole orientation
  - Concepts should be extensible to more complex trajectories and primitive bodies
- Five common types of mapping orbits considered
  - Terminator, ecliptic, and hover trajectories excel in a specific area, limited in others
  - Quasi-terminator and ping-pong provide more diverse observation opportunities across body
- Case study applied set of quantitative metrics to five candidate mapping orbits
  - Assumed spherical, phase-locked polyhedral body
- Mean quantities and the standard deviation of mean quantities are particularly insightful
  - Provide insight into local and global variety of observation geometries achieved
- Quantitative metrics confirm favorable mapping capabilities of quasi-terminator and ping-pong orbits this particular application

Quantifying Mapping Orbit Performance in the Vicinity of Primitive Bodies

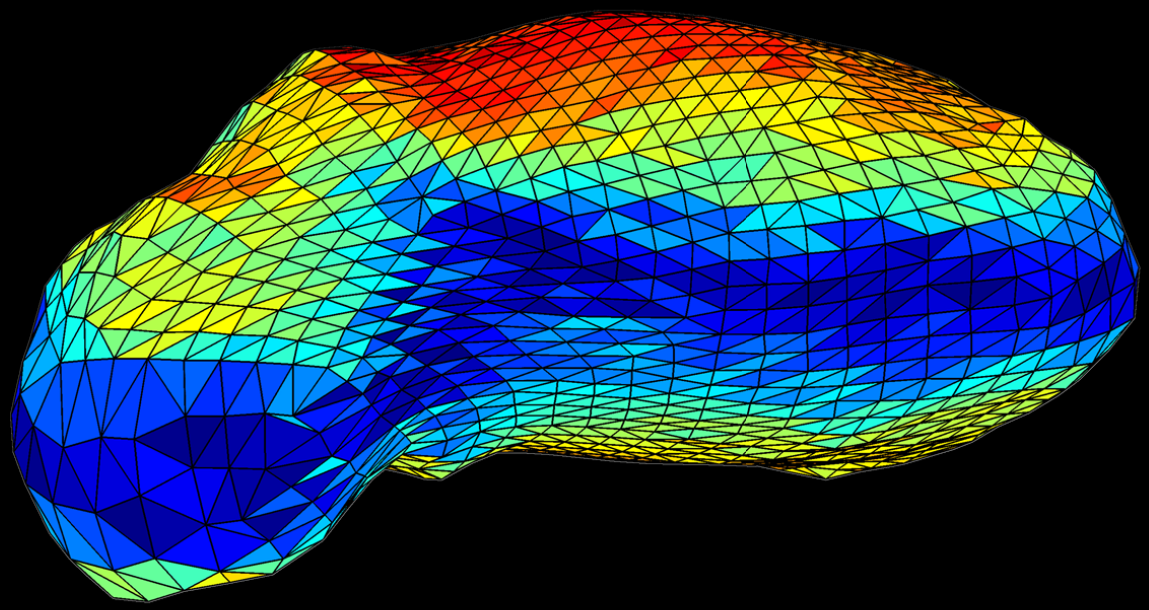

Thomas A. Pavlak, Stephen B. Broschart, and Gregory Lantoine

Jet Propulsion Laboratory, California Institute of Technology
Pasadena, California

© 2015 California Institute of Technology. Government sponsorship acknowledged.

Back-up Slides

Azimuth Angle

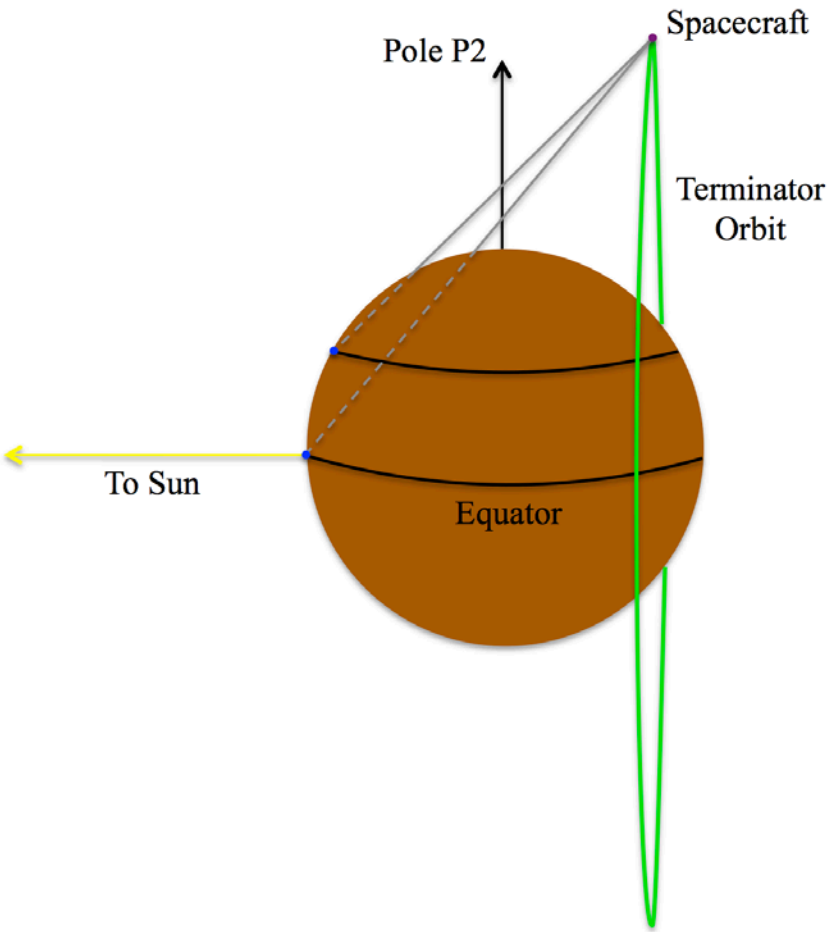

(a) Terminator orbit

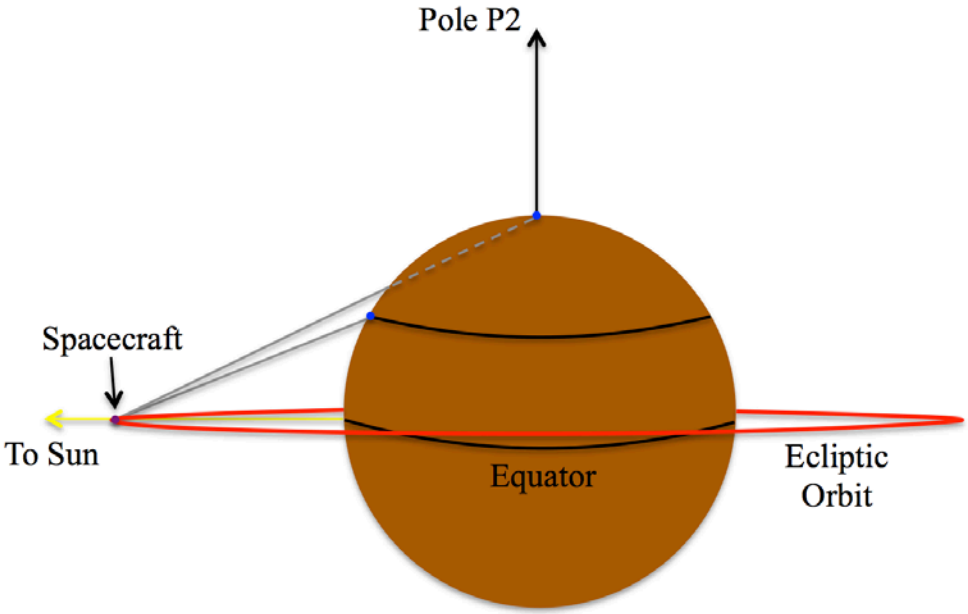

(b) Ecliptic orbit